Investigation on the accuracy and numerical dissipation when using the ULPH model for free-surface flows

Shi-Xian Wu, Peng-Nan Sun*, Xiao-Ting Huang
School of Ocean Engineering and Technology, Sun Yat-sen University
Zhuhai, China
sunpn@mail.sysu.edu.cn

Abstract — To improve the computational efficiency and reduce the excessive numerical dissipation, an extended support domain technique (ESDT) under the Updated Lagrangian particle hydrodynamics (ULPH) framework is proposed in this paper. A benchmark is tested to validate the superiority of the ULPH with ESDT. Results demonstrate that the ULPH with ESDT shows good accuracy, convergence, energy conservation, and high efficiency.

I. INTRODUCTION

Free surface flows are commonly observed in both nature (e.g. sea waves, tides, and floods) and engineering (e.g., liquid pipeline transportation, paint spraying, and jet washing). Particularly in ocean engineering, violent free surface flows (e.g., dam breaks, water entry, and liquid sloshing) always involve large deformation and highly nonlinear properties.

In order to deeply study these complex free surface flow problems, using the meshfree particle methods to accurately simulate these phenomena is widely acknowledged. Meshfree particle methods, such as the Smoothed Particle Hydrodynamics (SPH) methods, can naturally handle large free surface deformation and multi-phase interaction issues, meaning that they have a natural advantage in dealing with the free surface flows.

Although the traditional SPH model is successfully applied to various areas, there are still several critical issues that urgently need to be solved, including the high computational cost and excessive numerical dissipation. Generally, using fewer neighboring particles can directly enhance the efficiency, but at the cost of lower accuracy. According to Colagrossi et al. [1], fewer neighboring particles lead to excessive numerical dissipation, especially for long-term and long-distance simulations. To address this problem, kernel gradient correction (KGC) was carried out, and several new SPH models (such as δ-SPH^C [2, 3] which greatly overcomes the numerical dissipation) were proposed and gained promising results.

Recently, a novel meshfree Lagrangian particle method, called Updated Lagrangian particle hydrodynamics (ULPH), was proposed [4] and has been used for free-surface flows [5]. Considering that the structure of the discrete momentum equation of ULPH is similar to that of the δ-SPH^C model [2, 3], the ULPH scheme is applied to study and address the excessive numerical dissipation.

The present paper is constructed as follows. In Section 2, the ULPH scheme is briefly recalled, and subsequently an extended support domain technique (ESDT) under the ULPH framework is proposed. In Section 3, through analyzing the computational accuracy and the numerical dissipation, the superiority of the ULPH with ESDT is validated by comparing it with the SPH method. Finally, Section 4 concludes the present study.

II. METHODOLOGY

A. Governing equations of ULPH

The discrete governing equations [5] are written as follows:

$$\begin{cases} \dfrac{D\rho_i}{Dt} = -\rho_i \left\langle \nabla \cdot \boldsymbol{u} \right\rangle_i + \Phi_i \\ \dfrac{D\boldsymbol{u}_i}{Dt} = -\dfrac{1}{\rho_i}\left\langle \nabla p \right\rangle_i + \dfrac{1}{\rho_i}\boldsymbol{F}_{v,i} + \boldsymbol{g} \\ \dfrac{D\boldsymbol{r}_i}{Dt} = \boldsymbol{u}_i, \quad p_i = c_0^2\left(\rho_i - \rho_0\right), \quad V_i(t) = \dfrac{m_i}{\rho_i(t)} \end{cases} \tag{1}$$

where $\boldsymbol{u}$, p, and m represent the velocity vector, pressure, and mass of the particle, respectively. c_0 and ρ_0 are the artificial sound speed and background density, respectively. Φ_i is the density diffusive term, and $\boldsymbol{F}_{v,i}$ is the viscous term. More details can be found in the reference [5].

Through particle approximation, the differential operators of ULPH are expressed as follows [4]:

$$\begin{cases} \nabla(\bullet) = \sum_j W_{ij}\Delta(\bullet)\left(\boldsymbol{M}_i^{-1}\boldsymbol{r}_{ji}\right)V_j \\ \nabla\cdot(\bullet) = \sum_j W_{ij}\Delta(\bullet)\cdot\left(\boldsymbol{M}_i^{-1}\boldsymbol{r}_{ji}\right)V_j \end{cases} \tag{2}$$

in which W_{ij} is the WC2 kernel function. In this paper, kernel radius equals $2h$, where h is the smooth length. $\Delta(\bullet)$ represents $(\bullet)_j$ - $(\bullet)_i$, where i and j denote the target particle and neighboring particle, respectively. For example, $\Delta(\rho) = \rho_j - \rho_i$ and ρ is the density of the particle. $\boldsymbol{r}_{ji}$ represents $\boldsymbol{r}_j - \boldsymbol{r}_i$ and $\boldsymbol{r}$ is the position vector of the particle. V is the particle volume. $\boldsymbol{M}_i$ is the moment matrix of i, expressed as follows [4]:

$$\boldsymbol{M}_i = \sum_j W_{ij} \boldsymbol{r}_{ji} \otimes \boldsymbol{r}_{ji} V_j \tag{3}$$

Based on Equation (2) and Peridynamic theory, the $\langle \nabla \cdot \boldsymbol{u} \rangle_i$ and $\langle \nabla p \rangle_i$ in Equation (1) are written below [5]:

$$\begin{cases} \langle \nabla \cdot \boldsymbol{u} \rangle_i = \sum_j W_{ij} \left(\boldsymbol{u}_j - \boldsymbol{u}_i \right) \cdot \left(\boldsymbol{M}_i^{-1} \boldsymbol{r}_{ji} \right) V_j \\ \langle \nabla p \rangle_i = \sum_j W_{ij} \left(p_i \boldsymbol{M}_i^{-1} + p_j \boldsymbol{M}_j^{-1} \right) \boldsymbol{r}_{ji} V_j \end{cases} \tag{4}$$

Considering the matrix $\boldsymbol{M}$ may be ill-conditioned at the free-surface and its vicinity, the initial $\boldsymbol{M}$ in the above regions should be replaced by an optimal $\boldsymbol{M}'$ when calculating the governing equations, expressed as follows [5]:

$$\boldsymbol{M}_i' = \begin{bmatrix} \sum_j W_{ij} \left(x_j - x_i \right)^2 V_j & 0 & 0 \\ 0 & \sum_j W_{ij} \left(y_j - y_i \right)^2 V_j & 0 \\ 0 & 0 & \sum_j W_{ij} \left(z_j - z_i \right)^2 V_j \end{bmatrix} \tag{5}$$

B. *Extended support domain technique*

To increase the computational efficiency, a smaller smooth length h=1.35dx is used with the ULPH model, where dx is the initial particle distance. However, a smaller smooth length causes lower computational accuracy. To address this problem, a novel extended support domain technique (ESDT) is proposed in this paper. As shown in Fig. 1, one of the outermost neighboring particles (here j) of target particle i is discussed. Considering the differential operators, through replacing the matrix $\boldsymbol{M}_i^{-1}$ in the Equation (2) by $\left(\boldsymbol{M}_i^{-1} + \boldsymbol{M}_j^{-1} \right)/2$, the support domain radius of particle i is as if extended from conventional kh to approximately 2kh, since the matrix of particle j is calculated by its neighboring particles. As a result, owing to the decrease of smooth length, the computational cost effectively reduces. At the same time, thanks to the ESDT, the ULPH model remains relatively high in computational accuracy and low in numerical dissipation.

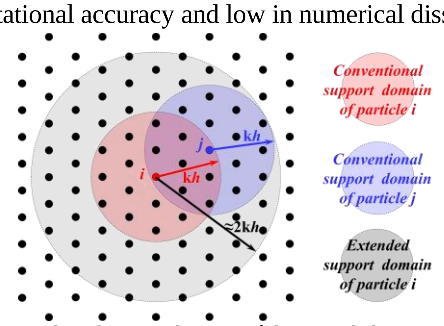

Figure 1. The schematic diagram of the extended support domain.

C. *Particle shifting technique*

Referring to the particle shifting technique (PST) proposed by Wang et al. [6], the PST of the ULPH scheme is applied in this paper, expressed as follows:

$$\delta \boldsymbol{u}_i = \begin{cases} -\mathrm{Ma} \cdot 2h \cdot c_0 \sum_j W_{ij} \left(1 + \chi_{ij} \right) \left(\dfrac{\boldsymbol{M}_i^{-1} + \boldsymbol{M}_j^{-1}}{2} \boldsymbol{r}_{ji} \right) V_j, \\ \text{if } i \text{ and all neighboring particle of } i \in \mathbb{I} \\ 0, \text{ if } i \in \mathbb{F} \\ -\mathrm{Ma} \cdot 2h \cdot c_0 \sum_j W_{ij} \chi_{ij} \left(\boldsymbol{M}_i^{-1} \boldsymbol{r}_{ji} \right) V_j, \text{ else and } \left| \boldsymbol{r}_{ji} \right| < l_i \end{cases} \tag{6}$$

where $\mathbb{I}$ and $\mathbb{F}$ represent the inner particle and free-surface particle. l_i is the smallest distance between i and the free-surface particle. χ_{ij} is written as follows:

$$\chi_{ij} = 0.2 \left(W_{ij} / W(dx) \right)^{0.4} \tag{7}$$

Referring to the consistent δ^+-SPH scheme [7], the governing equations of the ULPH with PST and ESDT are written below:

$$\begin{cases} \dfrac{D\rho_i}{Dt} = -\rho_i \langle \nabla \cdot \boldsymbol{u} \rangle_i - \rho_i \langle \nabla \cdot \delta \boldsymbol{u} \rangle_i + \langle \nabla \cdot (\rho \delta \boldsymbol{u}) \rangle_i + \Phi_i \\ \dfrac{D\boldsymbol{u}_i}{Dt} = -\dfrac{1}{\rho_i} \langle \nabla p \rangle_i + \langle \nabla \cdot (\boldsymbol{u} \otimes \delta \boldsymbol{u}) \rangle_i + \dfrac{1}{\rho_i} \boldsymbol{F}_{v,i} + \boldsymbol{g} \\ \dfrac{D\boldsymbol{r}_i}{Dt} = \boldsymbol{u}_i + \delta \boldsymbol{u}_i, \quad p_i = c_0^2 \left(\rho_i - \rho_0 \right), \quad V_i(t) = \dfrac{m_i}{\rho_i(t)} \end{cases} \tag{8}$$

in which $\langle \bullet \rangle_i$ is the particle approximation of $\bullet$. Based on Equation (2) and ESDT, $\langle \bullet \rangle_i$ in Equation (8) is written below:

$$\begin{cases} \langle \nabla \cdot \delta \boldsymbol{u} \rangle_i = \sum_j W_{ij} \left(\delta \boldsymbol{u}_j - \delta \boldsymbol{u}_i \right) \cdot \left(\boldsymbol{M}_i^{-1} \boldsymbol{r}_{ji} \right) V_j \\ \langle \nabla \cdot (\rho \delta \boldsymbol{u}) \rangle_i = \sum_j W_{ij} \left(\rho_j \delta \boldsymbol{u}_j + \rho_i \delta \boldsymbol{u}_i \right) \cdot \left(\dfrac{\boldsymbol{M}_i^{-1} + \boldsymbol{M}_j^{-1}}{2} \boldsymbol{r}_{ji} \right) V_j \\ \langle \nabla \cdot (\boldsymbol{u} \otimes \delta \boldsymbol{u}) \rangle_i = \sum_j W_{ij} \left(\boldsymbol{u}_j \otimes \delta \boldsymbol{u}_j + \boldsymbol{u}_i \otimes \delta \boldsymbol{u}_i \right) \cdot \left(\dfrac{\boldsymbol{M}_i^{-1} + \boldsymbol{M}_j^{-1}}{2} \boldsymbol{r}_{ji} \right) V_j \end{cases} \tag{9}$$

The $\langle \nabla p \rangle_i$ and $\langle \nabla \cdot \boldsymbol{u} \rangle_i$ are calculated based on Equation (4). Owing to the lack of neighboring particles in the free-surface and its vicinity, it should be noticed that the matrix $\boldsymbol{M}_i^{-1}$ is used to calculating $\langle \nabla \cdot \boldsymbol{u} \rangle_i$ and $\langle \nabla \cdot \delta \boldsymbol{u} \rangle_i$ in Equation (8) instead of $\left(\boldsymbol{M}_i^{-1} + \boldsymbol{M}_j^{-1} \right)/2$ to maintain the free-surface stability. Additionally, it is suggested to neglect the off-diagonal of the matrix $\boldsymbol{M}$ and take the average of the elements on the main diagonal of $\boldsymbol{M}$ to improve the stability when calculating the $\langle \nabla \cdot \boldsymbol{u} \rangle_i$ and $\langle \nabla \cdot \delta \boldsymbol{u} \rangle_i$.

III. RESULTS AND DISCUSSION

In this section, a benchmark, standing wave, is selected to validate the accuracy, conservation, and efficiency of the ULPH model with ESDT. The initial particle pressure and velocity are expressed as follows:

$$\begin{cases} u_i \big|_{t=0} = \varepsilon \dfrac{gkH}{2\omega} \dfrac{\cosh k y_i}{\cosh kH} \sin \left[k \left(x_i + \dfrac{L}{2} \right) \right] \\ v_i \big|_{t=0} = -\varepsilon \dfrac{gkH}{2\omega} \dfrac{\sinh k y_i}{\cosh kH} \cos \left[k \left(x_i + \dfrac{L}{2} \right) \right] \end{cases} \tag{10}$$

$$p_i \big|_{t=0} = \rho g \left(H - y_i \right) \tag{11}$$

in which u_i and v_i denote the X-axis and Y-axis velocities of particle i, respectively. x_i and y_i denote the horizontal and vertical coordinates. $\varepsilon = 2A/H$ represents the wave steepness, where A is the wave amplitude. In this paper, ε equals 0.1.

Wave number $k = 2\pi / \lambda$, where λ is wavelength and $\lambda = 1$ in this paper. ω is the angular frequency of wave and satisfies $\omega^2 = gk \tanh(kh)$. L=2 m and H=1 m are the length and height of the undisturbed water (see Fig. 2), respectively.

The initial pressure and velocity fields are shown in Fig. 2. A periodic boundary is applied on the left and right sides, and the bottom is a mirror boundary.

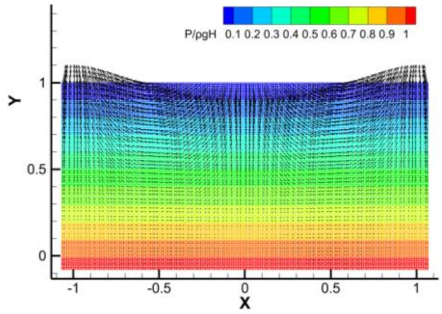

Figure 2. The initial pressure and velocity fields of the standing wave.

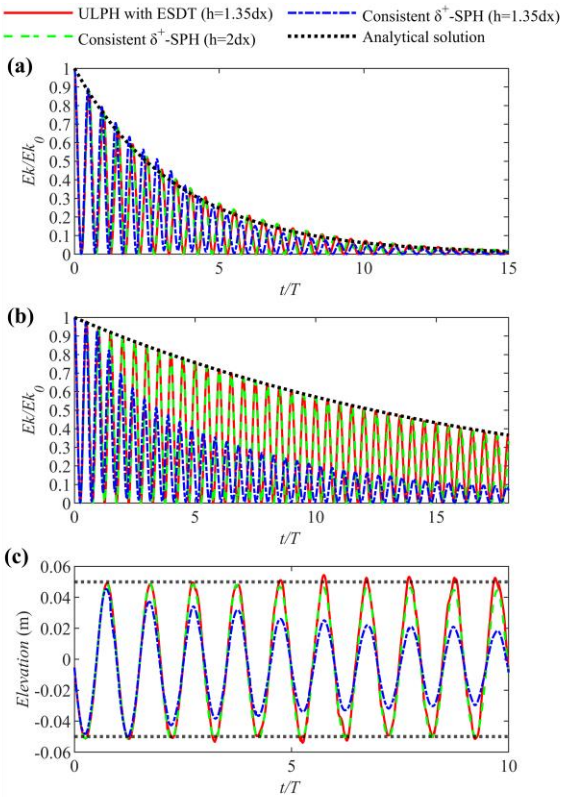

Figure 3. Comparison of the numerical dissipation between the ULPH with ESDT, the consistent δ^+-SPH[7], and the analytical solution. The Re of (a) and (b) are 500 and 2500, respectively. An inviscid fluid is considered in (c).

Two different Reynolds number, Re=500 and 2500, and an inviscid fluid are selected to discuss. Convergence was initially analysed. It is found that when the initial particle distance dx=H/100, the results converge and achieve a good balance between computational accuracy and cost. As shown in Fig. 3, when the smooth length h=1.35dx, the ULPH model with ESDT agrees well with the analytic solution and shows good accuracy, convergence, and energy conservation. On the contrary, the consistent δ^+-SPH shows wave over-attenuation and excessive numerical dissipation. When the smooth length of the consistent δ^+-SPH increases to 2dx, the result shows good accuracy and is similar to the ULPH with ESDT (h=1.35dx). Additionally, Fig. 3 shows that the energy conservation of the ULPH with ESDT is consistently superior, while the conservation of the consistent δ^+-SPH becomes weak as the Re increases, which is also reported in [1].

Subsequently, the computational efficiency is discussed. As shown in Table. 1, the first 100 steps and the first 1000 steps are considered. When the ULPH with ESDT (dx=H/100, h=1.35dx) and the consistent δ^+-SPH (dx=H/100, h=2dx) have similar accuracy, the former's efficiency is about 12.4% higher than that of the latter.

TABLE 1. COMPARISON COMPUTATIONAL EFFICIENCY BETWEEN THE ULPH WITH ESDT AND THE CONSISTENT DELTA-PLUS-SPH

Steps	**Computational Efficiency**	
	ULPH with ESDT (h=1.35dx)	***Consistent δ^+-SPH [7] (h=2dx)***
100	23 s	26 s
1000	217 s	250 s

IV. CONCLUSIONS

In this work, an extended support region technique (ESDT) is proposed under the ULPH framework to improve the computational efficiency and reduce the excessive numerical dissipation. Results indicate that when the smooth length is small, the ULPH model with ESDT shows good accuracy, convergence, energy conservation, and high efficiency, demonstrating that the ESDT effectively reduces discrete errors.

ACKNOWLEDGMENT

This research is supported by the Guangdong Basic and Applied Basic Research Foundation (No. 2024B1515020107); the National Natural Science Foundation of China (Grant No.52171329).

REFERENCES

[1] Colagrossi Andrea, et al. "Smoothed-particle-hydrodynamics modeling of dissipation mechanisms in gravity waves." *Physical Review E—Statistical, Nonlinear, and Soft Matter Physics* 87.2 (2013): 023302.

[2] Huang Xiao-Ting, et al. "Development of a numerical wave tank with a corrected smoothed particle hydrodynamics scheme to reduce nonphysical energy dissipation." *Chinese Journal of Theoretical and Applied Mechanics* 54.6 (2022): 1502-1515.

[3] Lyu Hong-Guan, et al. "Derivation of an improved smoothed particle hydrodynamics model for establishing a three-dimensional numerical wave tank overcoming excessive numerical dissipation." *Physics of Fluids* 35.6 (2023).

[4] Tu Qing-Song, and Li Shao-Fan. "An updated Lagrangian particle hydrodynamics (ULPH) for Newtonian fluids." *Journal of Computational Physics* 348 (2017): 493-513.

[5] Yan Jia-Le, et al. "Updated Lagrangian particle hydrodynamics (ULPH) modeling for free-surface fluid flows." *Computational Mechanics* 73.2 (2024): 297-316.

[6] Wang Ping-Ping, et al. "Improved particle shifting technology and optimized free-surface detection method for free-surface flows in smoothed particle hydrodynamics." *Computer Methods in Applied Mechanics and Engineering* 357 (2019): 112580.

[7] Sun Peng-Nan, et al. "A consistent approach to particle shifting in the δ-Plus-SPH model." *Computer Methods in Applied Mechanics and Engineering* 348 (2019): 912-934.